Meas. Sci. Technol. **21** (2010) 025205 (5pp) doi:10.1088/0957-0233/21/2/025205

A hybrid Fabry–Perot/Michelson interferometer sensor using a dual asymmetric core microstructured fiber

O Frazão[1,5], S F Silva[1], J Viegas[1], J M Baptista[1,2], J L Santos[1,3] and P Roy[4]

[1] INESC Porto—Instituto de Engenharia de Sistemas e Computadores do Porto, Rua do Campo Alegre 687, 4169-007 Porto, Portugal
[2] Centro de Competência de Ciências Exactas e da Engenharia, Universidade da Madeira, Campus da Penteada, 9000-390 Funchal, Portugal
[3] Departamento de Física da Faculdade de Ciências da Universidade do Porto, Rua do Campo Alegre 687, 4169-007 Porto, Portugal
[4] Xlim, Photonics Department, UMR 6172 CNRS University of Limoges, 123 Avenue Albert Thomas, 87060 Limoges, France

E-mail: ofrazao@inescporto.pt

Received 12 September 2009, in final form 11 November 2009
Published 6 January 2010
Online at stacks.iop.org/MST/21/025205

Abstract
A hybrid Fabry–Perot/Michelson interferometer sensor using a dual asymmetric core microstructured fiber is demonstrated. The hybrid interferometer presents three waves. Two parallel Fabry–Perot cavities with low finesse are formed between the splice region and the end of a dual-core microstructured fiber. A Michelson configuration is obtained by the two small cores of the microstructured fiber. The spectral response of the hybrid interferometer presents two pattern fringes with different frequencies due to the respective optical path interferometers. The hybrid interferometer was characterized in strain and temperature presenting different sensitivity coefficients for each topology. Due to these characteristics, this novel sensing head is able to measure strain and temperature, simultaneously.

Keywords: Fabry–Perot interferometer, Michelson interferometer, simultaneous measurement of strain and temperature

(Some figures in this article are in colour only in the electronic version)

Introduction

Fiber-optic interferometers based on Fabry–Perot (FP) and Michelson configurations have been developed for the measurement of different types of physical and chemical parameters [1–3]. These types of sensors present some advantages compared to other conventional sensors, namely high resolution, easy fabrication, simple configuration, good electromagnetic interference immunity and low cost.

The high resolution of these interferometers sensors is due to the sensitivity of the optical path. On the other hand, the optical path is very sensitive to several physical parameters, it being very difficult to make an interferometer tailored for sensing a specific physical measurement. One of the most common problems is the cross sensitivity to temperature. Several researchers have studied different techniques for simultaneous measurement of multi-parameters. A sensing head for simultaneous measurement of strain and temperature based on a Fabry–Perot cavity in a high birefringent fiber was proposed by Farahi *et al* in 1990 [4]. In 1994, Vengsarkar *et al* [5] proposed polarimetric and two-mode differential interferometric schemes incorporated in an elliptical-core fiber, which were able to resolve strain and temperature simultaneously. In the same year, the first sensing head using a Bragg grating structure able to discriminate strain and temperature was proposed and demonstrated by Xu *et al*

[5] Author to whom any correspondence should be addressed.

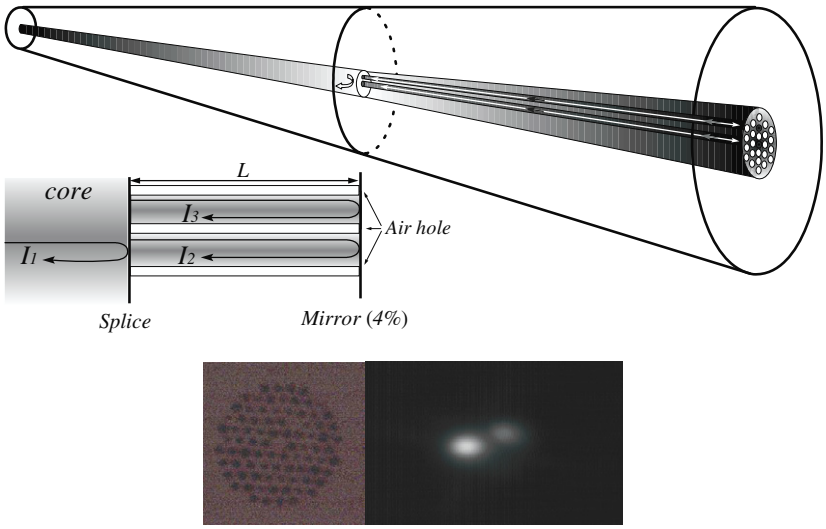

Figure 1. (*a*) Hybrid Fabry–Perot/Michelson interferometer sensor. (*b*) Cross section of the PCF. (*c*) Far-field intensity profile (at 1550 nm).

[6]. In 1996, Patrick *et al* [7] proposed the combination of two fiber Bragg gratings and a long-period grating for strain–temperature discrimination. A year after, Bhatia *et al* [8] presented a simultaneous strain–temperature measurement based on a single long-period grating. The combination of a Fabry–Perot cavity and a FBG [9, 10], and a configuration where the Fabry–Perot reflectors are FBGs [11] are also examples of structures aiming at such discrimination functionality through the combination of the Fabry–Perot concept and fiber grating devices. All these configurations can be used in several applications [12].

The traditional all-fiber Michelson interferometer consists of two optical fiber arms where temperature stability is difficult to obtain. Nevertheless, it is possible to make a Michelson interferometer using only one fiber. Swart *et al* [13] demonstrated a fiber modal interferometer in a Michelson configuration by forcing the light to cross the same long period grating twice and by mirroring the fiber end some distance after the grating. Recently, two Michelson interferometer configurations based on a taper have been presented. The first one uses the taper to inject the light in a two-core fiber [2], while the second work uses the taper to launch light in both fiber core and cladding [14].

In this work, we present a novel sensing head, in which the sensing region is a section of a microstructured fiber with two small cores. The Michelson interferometer is obtained by the simultaneous injection of light in the two cores by the single-mode fiber. The microstructured fiber end is cleaved and acts as a mirror. The two parallel Fabry–Perot interferometers are obtained between the two ends of the microstructured fiber. Indeed, due to the modal mismatch between the standard single-mode fiber core and the two microstructured fiber cores, as well as the cleaved end fiber, they both act as mirrors in the Fabry–Perot cavities.

Results

Figure 1 shows a scheme of the sensing head. The microstructured fiber presents two cores separated by one air hole and has a length of ∼11.5 mm. The main core (located in the center of the fiber) and the second core have similar diameters of ∼3 μm. The second core is formed due to the partial collapse of a hole, but still has an inner air hole of diameter ∼0.5 μm. The diameter of each air hole is 1.6 μm and the pitch is 2 μm, arranged in a triangular lattice. The hybrid cavity was illuminated with a broadband source at 1550 nm. An optical circulator was used to read the signal coming from the Fabry–Perot/Michelson interferometer. All the measurements were taken with an optical spectrum analyzer with a maximum resolution of 10 pm. Taking into account figure 1, and assuming two Fabry–Perot devices with low finesse, they can be modeled using the two-beam optical interference equation:

$$I_{\mathrm{FP1}} = I_1 + I_2 + 2\sqrt{I_1 I_2}\cos\left(\frac{4\pi n_1 L}{\lambda}\right) \tag{1}$$

$$I_{\mathrm{FP2}} = I_1 + I_3 + 2\sqrt{I_1 I_3}\cos\left(\frac{4\pi n_2 L}{\lambda}\right), \tag{2}$$

where $I_{\mathrm{FP}i}$ is the intensity of the interference signal of each Fabry–Perot, with $i = 1, 2$; I_1 is the first reflected intensity (splice region); I_2 and I_3 are the reflected intensities at the cavity end faces (end of the two cores), respectively; L is the cavity length; n_i ($i = 1, 2$) is the effective refractive index of the guided mode in each core and λ is the wavelength operation. For the Michelson interferometer, the equation can be given by

$$I_M = I_2 + I_3 + 2\sqrt{I_2 I_3}\cos\left(\frac{4\pi(n_1 - n_2)L}{\lambda}\right), \tag{3}$$

where I_M is the intensity of the interference signal. The intensity of the hybrid interferometer signal is obtained by $I_{\mathrm{hybrid}} = I_{\mathrm{FP1}} + I_{\mathrm{FP2}} + I_{\mathrm{M}}$, and comes out to be

$$I_{\mathrm{hybrid}} = 2[I_1 + I_2 + I_3] + 2\left[\sqrt{I_1 I_2}\cos\left(\frac{4\pi n_1 L}{\lambda}\right) + \sqrt{I_1 I_3}\cos\left(\frac{4\pi n_2 L}{\lambda}\right) + \sqrt{I_2 I_3}\cos\left(\frac{4\pi(n_1 - n_2)L}{\lambda}\right)\right]. \tag{4}$$

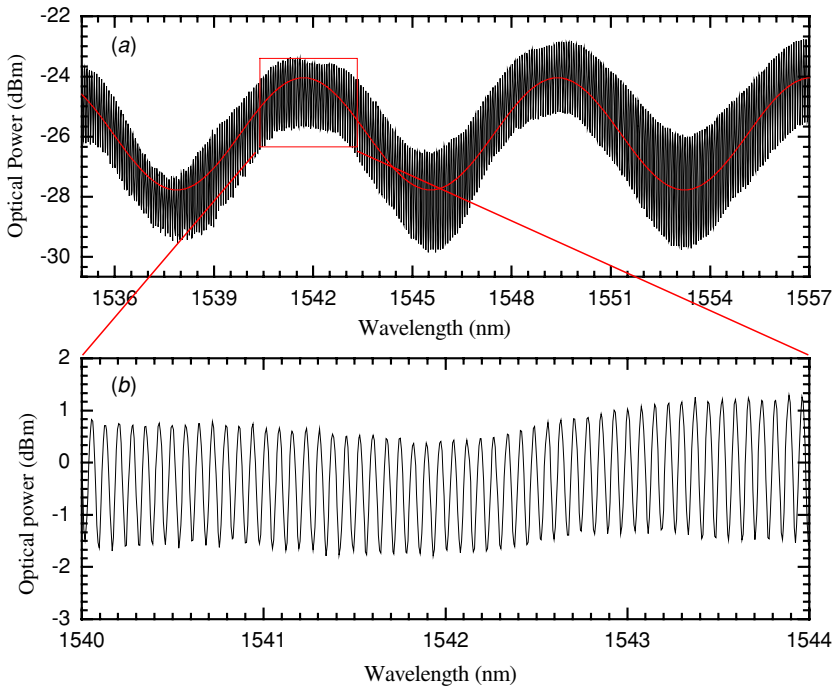

Figure 2. Spectral response of the hybrid FP/M interferometer sensor: (*a*) Michelson and (*b*) Fabry–Perot.

Figure 2(*a*) shows the spectral response of the hybrid interferometer, where the lower spatial frequency corresponds to the response of the Michelson interferometer with a spacing wavelength of 7.75 nm, showing a refractive index difference of 1.34×10^{-2}. In fact, if the two cores were equal, the refractive index difference would be zero. Nevertheless, the second core has a defect, a very small hole due to a partial hole collapse, which decreases its effective refractive index. This is the reason for the effective refractive index difference between the two Michelson arms. Taking a closer look at the signal interference, we can see the modulation of the two Fabry–Perot cavities. Figure 2(*b*) shows the pattern of fringes due to a small beat length between Fabry–Perot cavities. If the two Fabry–Perot cavities were illuminated with the same light intensity, a high beat length between the two interferences would be expected. In our setup, the principal core of the PCF is aligned with the center of the SMF28, while the second core is misaligned, receiving much lower light intensity. This unequal amplitude signal of the light launched in the two Fabry–Perot cavities produces a small beat length (see figure 1). The spacing wavelength of 0.074 nm in the principal modulation indicates a refractive index of 1.408.

The sensing head was characterized in strain at room temperature and for temperature without any applied strain. The sensing head was attached to a translation stage with a resolution of 1 μm and placed over a thermoelectric cooler device, which permits the temperature of the sensing head to be set with an error smaller than 0.1 °C.

Relative to the strain sensitivities ($K_{\varepsilon M}$, $K_{\varepsilon FP}$), the Michelson interferometer is insensitive to the applied strain. This insensitivity is expected since when the strain is applied, the two cores are simultaneously tensioned and the optical path variation is maintained constant, resulting in no change for the phase. In contrast, for the Fabry–Perot cavities, the optical path is modified because the length is increased when the strain is applied. Figure 3 shows the strain response for the hybrid interferometer.

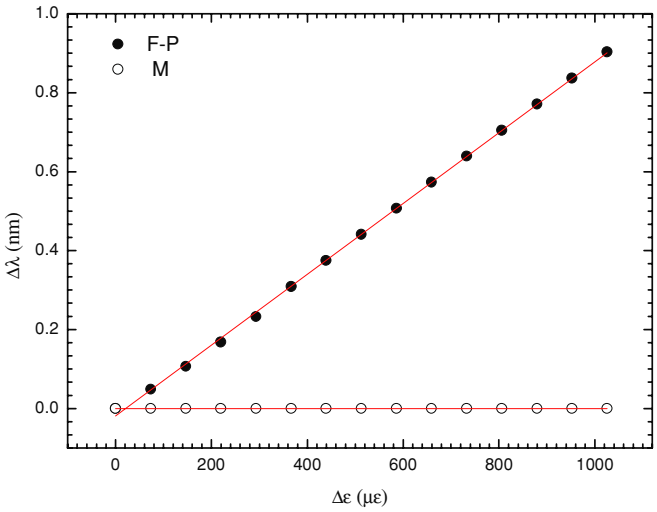

Figure 3. Strain response for the hybrid interferometer.

In what concerns the thermal sensitivities of the two interferometer types, they depend mostly on the thermo-optic coefficients of the fiber, which are essentially independent of the sensing head geometry. Due to the effective refractive index difference between the two cores, the Michelson configuration presents different thermal behavior when compared with the Fabry–Perot cavities where in this former case it is essentially determined by the thermo-optic coefficient

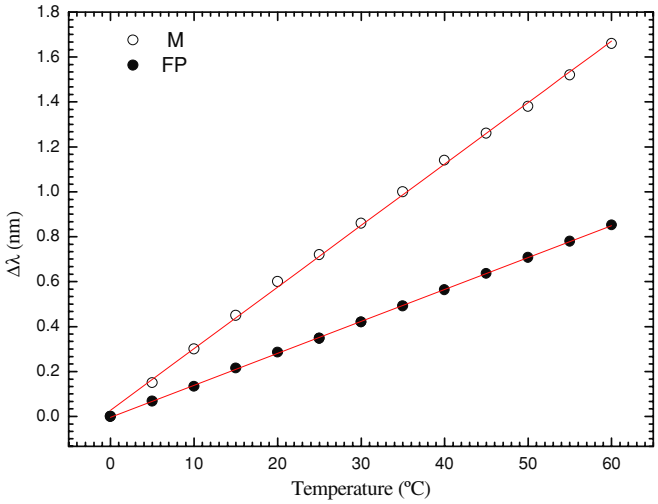

Figure 4. Temperature response for the hybrid interferometer.

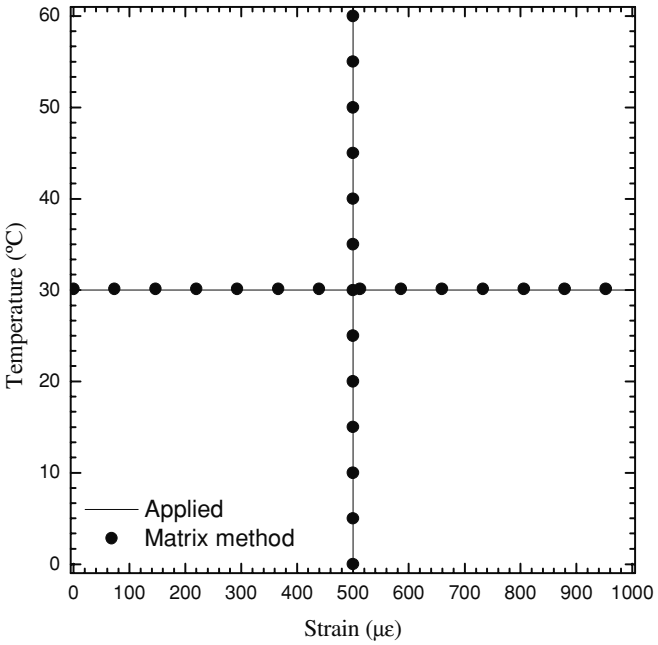

Figure 5. Sensor output as determined by the matrix method for applied temperature and strain.

Table 1. Strain and temperature sensitivity coefficients.

Interferometer	Strain sensitivity ($K_{\varepsilon M}$, $K_{\varepsilon FP}$) (pm $\mu\varepsilon^{-1}$)	Temperature sensitivity (K_{TM}, K_{TFP}) (pm $^{\circ}C^{-1}$)
Michelson	0 ± 0.05	27.38 ± 0.2
Fabry–Perot	0.89 ± 0.05	14.22 ± 0.5

of silica and, therefore, proportional to the cavity length. Indeed, it is expected that the temperature sensitivities (K_{TFP} and K_{TM}) are different, which was experimentally confirmed. Figure 4 shows the temperature response for the hybrid interferometer, and table 1 presents the values of the strain and temperature coefficients of the sensing head.

Using the strain and temperature coefficients, it is possible to write a well-conditioned system of two equations (5) for ΔT and $\Delta\varepsilon$, given in matrix form as

$$\begin{bmatrix}\Delta T\\ \Delta\varepsilon\end{bmatrix} = \frac{1}{D}\begin{bmatrix}K_{\varepsilon M} & -K_{\varepsilon FP}\\ -K_{TM} & K_{TFP}\end{bmatrix}\begin{bmatrix}\Delta\lambda_{FP}\\ \Delta\lambda_{M}\end{bmatrix}, \quad (5)$$

where the determinant is $D = -K_{\varepsilon FP}\ K_{TM}$. The matrix coefficients are obtained from the experimental slopes shown in figures 3 and 4, resulting in

$$\begin{bmatrix}\Delta T\\ \Delta\varepsilon\end{bmatrix} = -\frac{1}{24.36}\begin{bmatrix}0 & -0.89\\ -27.38 & 14.22\end{bmatrix}\begin{bmatrix}\Delta\lambda_{FP}\\ \Delta\lambda_{M}\end{bmatrix}. \quad (6)$$

The performance of this technique was evaluated when the sensing head undertook strain variations in a range of 1000 $\mu\varepsilon$ at a fixed temperature ($\Delta T = 30\ ^{\circ}C$) and the other way around, i.e. temperature variations in a range of 60 $^{\circ}C$ for a specific applied strain ($\Delta\varepsilon = 500\ \mu\varepsilon$). The results are expressed in figure 5, from where rms deviations relative to the applied values of $\pm 0.3\ ^{\circ}C$ and $\pm 0.3\ \mu\varepsilon$ for temperature and strain, respectively, are obtained.

Conclusions

In summary, a hybrid Fabry–Perot/Michelson interferometer for simultaneous measurement of strain and temperature was proposed. The sensing head is formed by 11.5 mm of a microstructured fiber with a dual core structure. Due to different behavior of the interferometers, different strain and temperature sensitivities were obtained. This configuration can be applied in different engineering areas and can also be used to discriminate other physical or chemical parameters.

Acknowledgments

This work was supported by the COST 299—Optical Fibres for New Challenges Facing the Information Society. The authors would also like to thank the FCT/CNRS 2009–2010 by the project SOFIA.

References

[1] Yuan L, Yang J, Liu Z and Sun J 2006 In-fiber integrated Michelson interferometer *Opt. Lett.* **31** 2692
[2] Chen Y and Taylor H F 2002 Multiplexed fiber Fabry–Perot temperature sensor system using white-light interferometry *Opt. Lett.* **27** 903
[3] Choi H Y, Park K S, Park S J, Paek U-C, Lee B H and Choi E S 2008 Miniature fiber-optic high temperature sensor based on a hybrid structured Fabry–Perot interferometer *Opt. Lett.* **33** 2455
[4] Farahi F, Webb D J, Jones J D C and Jackson D A 1990 Simultaneous measurement of temperature and strain: cross-sensitivity considerations *J. Lightwave Technol.* **8** 138
[5] Vengsarkar A M, Michie W C, Jankovic L, Culshaw B and Claus R O 1994 Fiber-optic dual-technique sensor for simultaneous measurement of strain and temperature *J. Lightwave Technol.* **12** 170
[6] Xu M G, Archambault J-L, Reekie L and Dakin J P 1994 Discrimination between strain and temperature effects using dual-wavelength fibre grating sensors *Electron. Lett.* **30** 1085

[7] Patrick H J, Williams G M, Kersey A D, Pedrazzani J R and Vengsarkar A M 1996 Hybrid fiber Bragg grating/long period fiber grating sensor for strain/temperature discrimination *IEEE Photonics Technol. Lett.* **8** 1223

[8] Bhatia V, Campbell D and Claus R O 1997 Simultaneous strain and temperature measurement with long-period grating *Opt. Lett.* **22** 648

[9] Lui T, Fernando G F, Zhang L, Bennion I, Rao Y J and Jackson D A 1997 Simultaneous strain and temperature measurement using a combined fibre Bragg grating/ extrinsic Fabry–Perot *12th Int. Conf. Optical Fibre Sensors (OFS 1997) (Williamsburg, USA)* pp 28–31, 40

[10] Rao Y J, Zeng X K, Wang Y P, Zhu T, Ran Z L, Zhang L and Bennion I 2001 Temperature–strain discrimination using a WDM chirped in-fibre-Bragg-grating and extrinsic Fabry–Perot *Chin. Phys. Lett.* **18** 643

[11] Du W-C, Tao X-M and Tam H-Y 1999 Fiber Bragg grating cavity sensor for simultaneous measurement of strain and temperature *IEEE Photonics Technol. Lett.* **11** 105

[12] Ferraro P and De Natale P 2002 On the possible use of optical fiber Bragg gratings as strain sensors for geodynamical monitoring *Opt. Lasers Eng.* **37** 115–30

[13] Swart P L 2004 Long-period grating Michelson refractometric sensor *Meas. Sci. Technol.* **15** 1576

[14] Frazão O, Caldas P, Araújo F M, Ferreira L A and Santos J L 2007 Optical flowmeter using a modal interferometer based on a single nonadiabatic fiber taper *Opt. Lett.* **32** 1974